

To cite this article: YU Y, GUO H, YU J X, et al. Study on ultimate bearing capacity of unconventional stepped deck in cruise ship [J/OL]. Chinese Journal of Ship Research, 2023, 18(6). <http://www.ship-research.com/en/article/doi/10.19693/j.issn.1673-3185.02994> (in both Chinese and English).

DOI: 10.19693/j.issn.1673-3185.02994

Study on ultimate bearing capacity of unconventional stepped deck in cruise ship



YU Yang^{1,2}, GUO Hu^{1,2}, YU Jianxing^{1,2}, WANG Fucheng^{1,2}, ZHANG Lingbo^{1,2}, SU Yefan^{1,2}

1 State Key Laboratory of Hydraulic Engineering Intelligent Construction and Operation, School of Civil Engineering, Tianjin University, Tianjin 300072, China

2 Tianjin Key Laboratory of Port and Ocean Engineering, School of Civil Engineering, Tianjin University, Tianjin 300072, China

Abstract: [Objective] In order to determine the strength of the special deck structure of a cruise ship, this study investigates the ultimate bearing capacity of an unconventional stepped deck used in the layout of the cruise theater. [Methods] Based on the quasi-static ABAQUS method, the ultimate bearing capacity of a stepped deck is calculated and the weak positions of the structure are determined and compared with conventional deck failure modes. Meanwhile, the influence of the deck, longitudinal frame, girder web and girder panel thickness on the ultimate bearing capacity of the structure are investigated, and two structural optimization ideas are proposed: pillar reinforcement and longitudinal reinforcement. [Results] The results show that the failure of the stepped deck mainly occurs at the boundary of the layer with the largest height difference; the ultimate bearing capacity of the stepped deck decreases significantly compared with that of a conventional deck; and the corresponding compression displacement and collapse depth increase obviously. The ultimate bearing capacity increases with the thickness of the deck, longitudinal frame, girder web and girder panels, and the improvement effect of girder web thickness is the most significant. The ultimate bearing capacity of the structure can be effectively improved by adding pillars or increasing the height of the web in the weak position of the structure. [Conclusion] This study has great significance for the design and optimization of special decks for modern cruise ships.

Key words: cruise ship; stepped deck; ultimate bearing capacity; structure optimization

CLC number: U661.43

0 Introduction

As a burgeoning high-value-added vessel, a luxury cruise ship has the potential to yield substantial economic and social advantages. Nevertheless, the plethora of functions not only elevates the complexity of design but also imposes more stringent demands on the structural strength of the hull. At present, the limit state method is favored as a replacement for the allowable stress method in the structural design and strength

assessment of ships^[1]. Traditional normative design typically employs the permissible stress method, operating under the belief that as long as the requirements of permissible stress are met, the structure will not undergo failure. Nevertheless, this method falls short in assessing the ultimate bearing capacity of the structure and is unable to determine the margin of safety of the said structure. In contrast, the limit state method proves more advantageous as it can authentically reflect the ultimate strength of the hull structure. Moreover, it

Received: 2022 - 07 - 01

Accepted: 2022 - 10 - 21

Supported by: High-tech Ships Research Program of Ministry of Industry and Information Technology (MC-201917-C09)

Authors: YU Yang, male, born in 1988, Ph.D., associate professor. Research interests: Reliability and hydrodynamics of marine structures. E-mail: yang.yu@tju.edu.cn

GUO Hu, male, born in 1998, master's degree candidate. Research interests: Structural strength and dynamic response of ships. E-mail: hu_guo@tju.edu.cn

YU Jianxing, male, born in 1958, Ph.D., professor. Research interests: Reliability research and risk assessment of marine structures

***Corresponding author:** YU Jianxing

enables minimizing the weight of the hull while ensuring the safety of the structure. Therefore, studying the ultimate strength of the hull structure holds great significance in ensuring the safety of the hull structure and enhancing its overall economic efficiency.

The ultimate strength of stiffened plates, being a pivotal stress structure in ship hulls, has garnered significant attention from scholars both domestically and internationally. Paik et al. [2-3] conducted a study on outer bottom stiffened-plate structures of double-hull ships. They selected a model with a "1/2 + 1 + 1/2" strong member span and examined the influence of initial imperfections, loading types, and computational techniques on the ultimate bearing capacity of the structure. In Cui et al.'s study [4] on the ultimate strength of container ships, they summarized empirical formulas for the initial deflection deformation of the stiffened plate. Additionally, they calculated the ultimate bearing capacity of the stiffened plate under the combined action of axial pressure and lateral seawater pressure. Liu et al. [5] delved into the impact of structural openings on strength. They conducted an analysis of the failure behavior of longitudinal girders with large openings in the deck and perforated high webs using both finite element simulations and experiments. Simultaneously, Liu et al. [6] conducted an in-depth study on the buckling and ultimate strength of long-span decks with their progressive collapse processes. Wan et al. [7], through a discussion on the stability of longitudinal compression in long-span decks, introduced the optimization design concept for deck grillage. Zhang et al. [8] calculated the ultimate strength under complex loading by taking into account the effects of model range and initial imperfections on the ultimate bearing capacity of the stiffened plate. Guo [9] calculated the ultimate bearing capacity of a cruise ship high web frame through testing and finite element simulations. They also explored the effect of different ratios of web openings on the structure. Gan et al. [10] investigated the failure mode and ultimate strength of perforated high web decks in cruise ship superstructures. Zhou et al. [11] simulated the ultimate bearing capacity under axial pressure of two forms of double deck frame with simultaneous openings in the deck and broadside, as well as double openings in the deck through tests. They also summarized the collapse pattern of multi-opening decks.

In summary, significant progress has been made in researching the ultimate bearing capacity of stiffened plates. However, the focus has primarily been on conventional decks and plate frame structures, including those with openings, long spans, and high webs derived from such configurations. Nevertheless, as ship functionality continues to evolve, unconventional plate frames are gradually finding their way into ship designs. Examples include the stepped deck utilized in the theater and cinema arrangements of medium- and large-sized cruise ships. The study of the ultimate strength of these unconventional plate frames holds practical significance. In light of this, the paper will undertake a study on the strength of unconventional stepped decks in cruise ships. Through a comparative analysis with conventional decks of equal size, the aim is to summarize the structural failure characteristics and propose ideas for structural optimization design.

1 Numerical model

1.1 Model size and material properties

Fig. 1 illustrates the deck structure of the cruise ship theater. The stepped deck model was established based on the actual size of the drawings as shown in Fig. 2. The model is 20.6 meters long and 18.2 meters wide, featuring a total of 7 steps designated as T0 to T6. The height difference from T0 to T1 is 750 mm, and the height difference from T1 to T6 is 150 mm. The deck longitudinal spacing is 700 mm, and along the ship's length, 4 T-shaped longitudinal girders of dimensions 450×8/150×10 are arranged. The longitudinal modeling is simplified to a 150×7 lath structure. *AB* and *MN* represent the deck edges, and the entire structure employs simulation by using S4R four-node shell element. Reduced integration is utilized in the operational process.

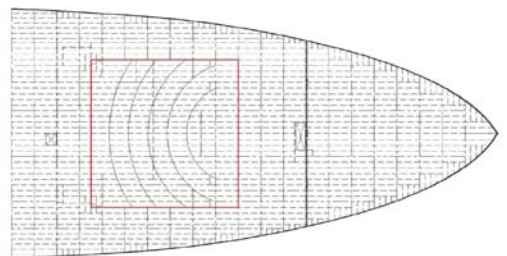


Fig. 1 Deck structure of cruise theatre

In accordance with the requirements of the CCS rules [12], the section modulus (W) and moment of

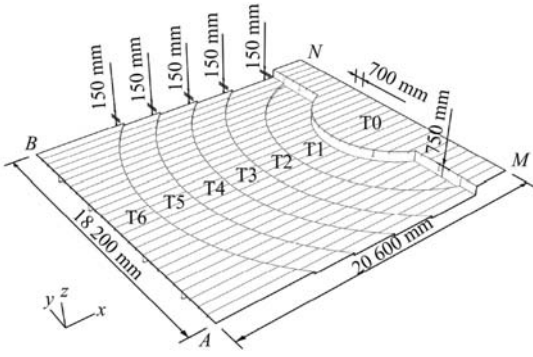


Fig. 2 3D model drawing of stepped deck

inertia (I) of the primary supporting members of the strength deck structure and the lower deck structure must satisfy the following relationship:

$$W \nless 5Shl^2K \tag{1}$$

$$I \nless 2Wl/K \tag{2}$$

where S is the spacing of the primary supporting members, h is the deck indentation head, l is the span of the primary supporting members, and K is the material coefficient.

Due to the unique characteristics of the structure, the spacing and span of longitudinal girders are not completely equidistant. When calculating the moment of inertia as per the specifications, the maximum value of each structural parameter is considered. Therefore, the required moment of inertia for the longitudinal girder is $I \nless 10 \times 5.6 \times 0.45 \times 4.413^3 = 2\,166\text{ cm}^4$. The moment of inertia for the longitudinal girder used in this paper is $11\,677\text{ cm}^4$, meeting the specification requirements.

The structure is constructed using high-strength steel with the following properties: density $\rho = 7\,850\text{ kg/m}^3$, modulus of elasticity $E = 2.06 \times 10^{11}\text{ Pa}$, Poisson's ratio $\nu = 0.3$, and yield strength $\sigma_y = 355\text{ MPa}$. The bilinear elastic-plastic material model [13] was selected for plasticity properties, with the modulus after yielding denoted as $E_h = 1 \times 10^9\text{ Pa}$.

1.2 Initial imperfection setting

The initial deflection deformation of the stiffened plate is bound to occur during the welding process, and the presence of initial imperfections will impact the ultimate strength of the plate frame. The initial imperfections of the plate frame encompass three types[14]: the overall initial deflection of the plate frame ω_{opl} , the initial deflection of the stiffener beam-column type ω_{oc} , and the initial deflection of the stiffener lateral inclination type ω_{os} , namely

$$\omega_{opl} = A_0 \sin\left(\frac{m\pi x}{a}\right) \sin\left(\frac{\pi y}{b}\right) \tag{3}$$

$$\omega_{oc} = B_0 \sin\left(\frac{\pi x}{a}\right) \sin\left(\frac{\pi y}{b}\right) \tag{4}$$

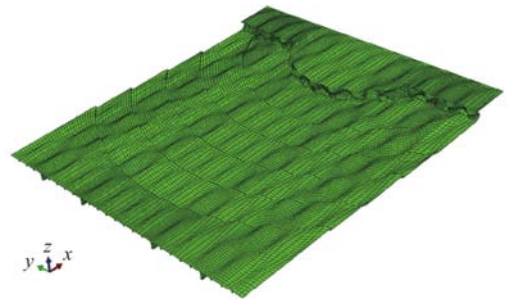
$$\omega_{os} = C_0 \frac{z}{h_w} \sin\left(\frac{\pi x}{a}\right) \tag{5}$$

where A_0 , B_0 , and C_0 represent the respective initial deflection amplitudes, where $A_0 = 0.1\beta^2 t$, $B_0 = C_0 = 0.0015a$, with a being the transverse member spacing, b the longitudinal member spacing, t the thickness of the plate frame, m the buckling half-wave number of the plate frame, and h_w the height of the stiffener.

The flexibility coefficient (β) of the plate frame is

$$\beta = \frac{b}{t} \sqrt{\frac{\sigma_y}{E}} \tag{6}$$

During the calculation process, the field function is employed to apply the three initial imperfections to the corresponding mesh nodes in the form of displacement loads. The resultant file is then calculated and re-imported as the initial state for subsequent calculations. The stepped deck, after incorporating the initial deflection deformation, is depicted in Fig. 3.



(a) Front side of stepped deck



(b) Reverse side of stepped deck

Fig. 3 The initial deformation after the effect is magnified by ten times

1.3 Loads and boundary conditions

In this paper, the ultimate bearing capacity of the stepped deck is calculated using the ABAQUS quasi-static method. All the nodes of the deck edges AB and MN are coupled to the midpoints of the corresponding edges $RP1$ and $RP2$, respectively.

The boundary conditions $U_y = 0$, $U_z = 0$, $UR_x = 0$, $UR_z = 0$ are imposed on all four edges. Additionally,

free constraints are set for the longitudinal displacement along the x -axis and rotation along the y -axis. Subsequently, displacement loads are simultaneously applied to the coupling points $RP1$ and $RP2$ in the same direction with equal magnitude. This is done to simulate the total longitudinal bending pressure on the plate frame along the ship's length. Finally, force and displacement data of the coupling points are extracted.

1.4 Mesh convergence analysis

The results of the mesh convergence analysis are

Table 1 Results of convergence analysis

Program	Number of meshes N						Ultimate bearing capacity/kN	Relative error/%
	N_{AB}	N_{BN}	N_G	N_{HF}	N_{HM}	N_{SUM}		
Mesh 1	78	104	2	6	2	22 208	4 318	11.37
Mesh 2	108	104	2	6	2	26 735	4 053	4.54
Mesh 3	108	104	3	9	4	33 492	3 877	
Mesh 4	156	104	3	9	4	41 355	3 771	-2.73

2 Analysis of results

2.1 Ultimate bearing capacity of stepped deck

Utilizing the numerical calculation with the aforementioned model, Fig. 4 illustrates the changes in internal energy and kinetic energy throughout the entire process. Ultimately, the load-displacement curve of the stepped deck after compression is obtained and presented in Fig. 5. From Fig. 5, it is observed that as the longitudinal compression displacement increases, the force on the deck also rises. When the displacement of the compressed side reaches 13 cm, the structure attains the ultimate strength state, and the corresponding ultimate bearing capacity $F_{max} = 3\ 877$ kN. After surpassing the limit state, the load-carrying capacity of the deck experiences a slight decrease and then stabilizes in a relatively smooth state. Combining with Fig. 6, the stress and displacement contours of the ultimate strength state of the stepped deck reveal that the failure primarily occurs at the junction of T0 and T1 after compression. The maximum drop depth of the collapse center is more than 0.62 m. Simultaneously, longitudinal girders of each step exhibited varying degrees of deformation. Notably, the two longitudinal girders at the center of T0 displayed significant lateral yielding.

presented in Table 1. Here, N_{AB} and N_{BN} denote the number of elements of the stepped deck along the ship's width and length, respectively; N_G is the number of elements in the direction of longitudinal height; N_{HF} and N_{HM} are the number of elements in the direction of longitudinal girder web height and panel width, respectively. N_{SUM} represents the total number of elements. As observed from Table 1, the results of the ultimate bearing capacity calculation show a tendency to converge with the gradual increase in the number of meshes. To attain high computational efficiency and accuracy, mesh 3 is ultimately chosen for the calculation.

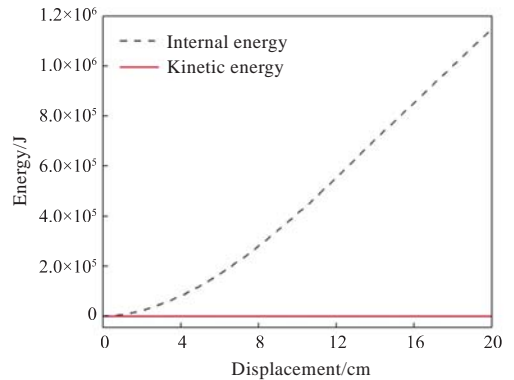


Fig. 4 Energy curve

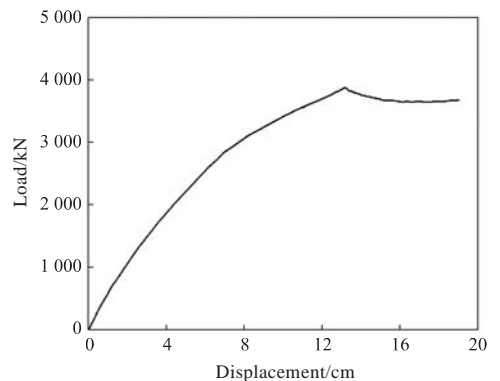
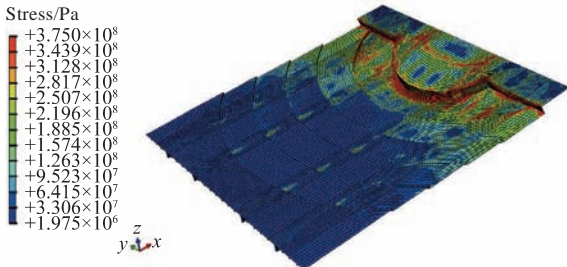


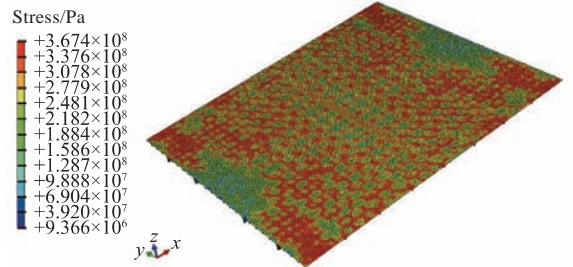
Fig. 5 Load-displacement curve

2.2 Comparison of failure modes

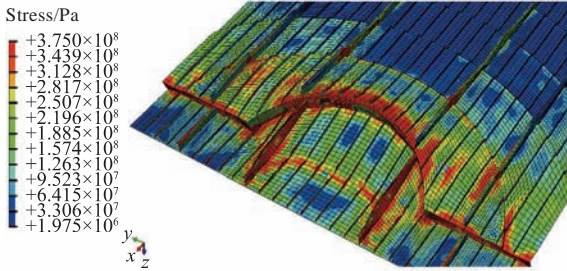
To gain a clearer understanding of failure characteristics of the stepped deck, a comparative analysis is conducted with the conventional long-span deck. The settings of geometrical dimensions,



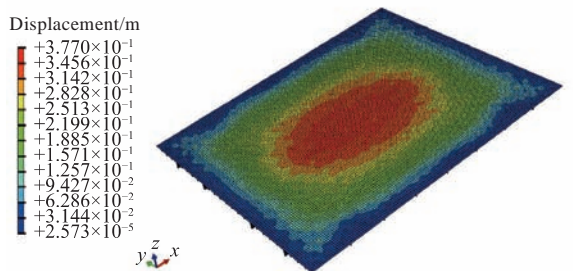
(a) Stress contours of front side of stepped deck



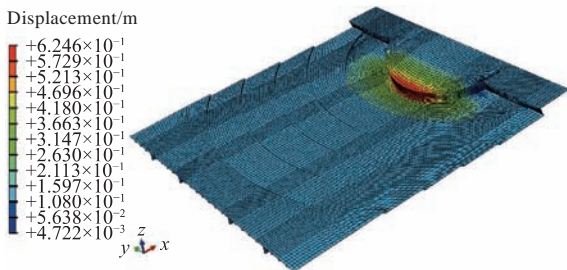
(a) Stress contours



(b) Stress contours of reverse side of stepped deck



(b) Displacement contours



(c) Displacement contours

Fig. 6 Ultimate strength state of stepped deck

Fig. 7 Ultimate strength state of conventional deck

Table 2 Comparison of ultimate strength between stepped deck and conventional deck

	Longitudinal compression displacement/cm	Ultimate bearing capacity/kN	Depth of collapse center/m
Stepped deck	13.2	3 877	0.62
Conventional deck	2.1	20 774	0.37

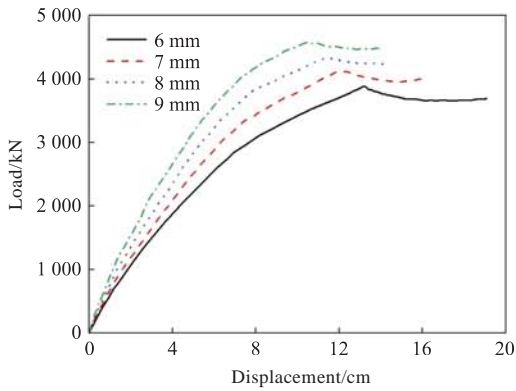
2.3 Effects of structural parameters

material parameters, boundary conditions, and initial imperfections of the conventional deck are consistent with those of the stepped deck during the calculation process.

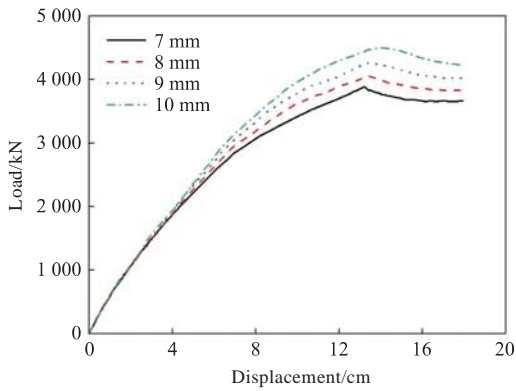
Comparing Fig. 6 and Fig. 7, it is found that the compressive failure mode of the conventional deck exhibits a regular symmetric distribution. The main occurrence is block yielding between panels, with the collapse initiating from the geometric center and radiating outward. On the other hand, the stepped deck designates the junction of T0 and T1 with the largest height difference as the collapse center. The high-stress region is primarily concentrated at the junction of each step, manifesting in the form of ring yielding. Meanwhile, by comparing the data in Table 2, it is found that the ultimate bearing capacity of the stepped deck decreases significantly compared with that of the conventional deck of the same size. It is only about 20% of the conventional deck, and the longitudinal compression displacement corresponding to the ultimate strength state and the depth of the collapse center also increase significantly.

To further elucidate the impact of different structural parameters on the ultimate bearing capacity, while maintaining the structural geometry unchanged, the study investigates the effect of altering the thickness of the deck, longitudinal, longitudinal girder web, and longitudinal girder panel on the ultimate bearing capacity of the stepped deck. With an increment of 1 mm thickness, the strength calculation is performed for decks with thickness ranging from 6 mm to 9 mm, longitudinals from 7 mm to 10 mm, longitudinal girder webs from 8 mm to 11 mm, and longitudinal girder panels from 10 mm to 13 mm. The results are presented in Fig. 8.

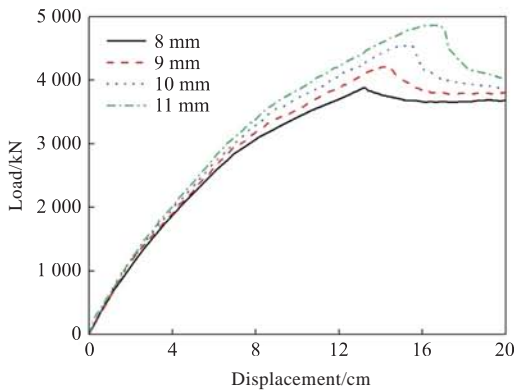
From Fig. 8, it is observable that the ultimate bearing capacity of the structure increases with the thickness of the deck, longitudinal, longitudinal girder web, and longitudinal girder panel increasing. However, the increase in deck thickness results in a decrease in displacement corresponding to the ultimate strength state. On the other hand, the increase in the other three parameters leads to an increase in displacement corresponding to the ultimate strength state. This indicates that the



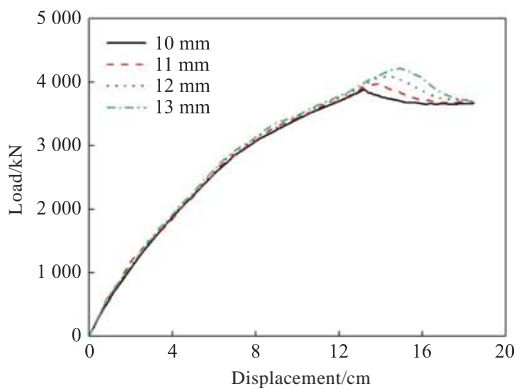
(a) Deck plate thickness effect



(b) Longitudinal plate thickness effect



(c) Effect of longitudinal girder web plate thickness



(d) Effect of longitudinal girder panel plate thickness

Fig. 8 Influence of structural parameter change of stepped deck

structure's ability to resist deformation is enhanced along with the increase in ultimate bearing capacity. In addition, from Fig. 8 (d), it is observable that the

change in plate thickness of the longitudinal girder panel has little effect on the force before the structure reaches the limit state. It primarily increases the ultimate bearing capacity of the structure and the displacement corresponding to the limit state. Conversely, the increase in the other three parameters will also elevate the force before the limit state of the structure. In terms of the effect, when the deck thickness increases from 6 mm to 9 mm, the ultimate bearing capacity of the structure rises by 686 kN. Similarly, an increase in longitudinal thickness from 7 mm to 10 mm results in a 625 kN increase in ultimate bearing capacity. Moreover, an increase in longitudinal girder web thickness from 8 mm to 11 mm leads to a 980 kN increase, and an increase in longitudinal girder panel thickness from 10 mm to 13 mm also results in a 342 kN increase in ultimate bearing capacity.

Relative to the original structure, the percentage increase in the ultimate bearing capacity of the stepped deck resulting from changes in the thickness of decks, longitudinals, longitudinal girder webs, and longitudinal girder panels is calculated as shown in Fig. 9. The analysis reveals that when the plate thicknesses are uniformly increased in 1 mm increments, the change in the longitudinal girder web has the most significant effect on enhancing the ultimate bearing capacity, with an increase of more than 25%. The enhancement effects of the deck and longitudinal are both around 16%, while the improvement resulting from the change in the longitudinal girder panel is the most limited with only 8%.

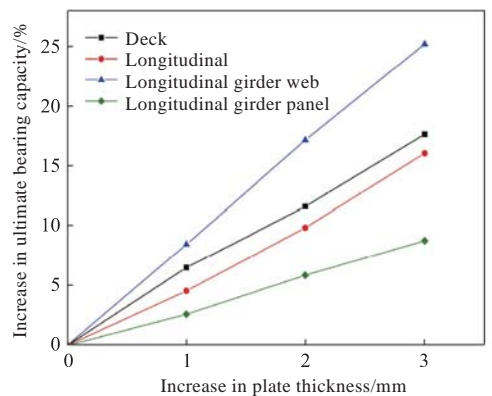


Fig. 9 Increase curve of ultimate bearing capacity

3 Structural strengthening and optimization

The above numerical calculations and analyses provide insights into the weak position of the cruise ship stepped deck structure and the impact of

structural parameter changes on the ultimate bearing capacity. From a structural perspective, two strengthening schemes are proposed: pillar strengthening and longitudinal girder strengthening, as shown in Fig. 10.

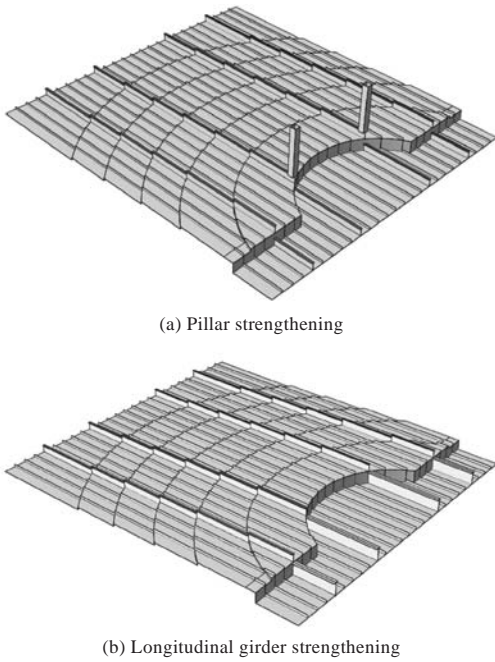


Fig. 10 Stepped deck structural optimization

The pillar strengthening involves adding two 3 m long square pillars at the junction of T0 and T1 to limit vertical displacement during deformation. On the other hand, the longitudinal girder strengthening entails increasing the height of the longitudinal girder web at T0 and widening the corresponding longitudinal girder panels from 150 mm to 300 mm. This aims to reduce the instability of the high web. Simultaneously, to further assess the efficiency of the strengthening schemes, calculations were performed for three sizes of pillars and longitudinal girders. These results were then compared with the original structure, and the findings are presented in Table 3 and Table 4.

The stress results for the pillar size 350×12 and longitudinal girder size 750×8/300×10 at T0 are illustrated in Fig. 11. Combined with Table 3, it is found that the pillar strengthening effectively enhances the ultimate bearing capacity of the structure while causing a slight increase in the total weight of the structure. Moreover, the larger the pillar size, the greater the ultimate bearing capacity of the structure. Nevertheless, enlarging the pillar size will inevitably occupy space on the lower deck, impacting the functionality of the cruise ship. Combined with Table 4, it is found that the longitudinal girder strengthening significantly

improves the ultimate bearing capacity of the structure. However, a higher level of longitudinal girder strengthening does not necessarily yield better results. Upon comparison, it is found that when the height of the longitudinal girder at T0 is elevated to that of the deck at T1 (750 mm), the ultimate bearing capacity of the structure increases by 35.8%, marking the most significant improvement. Meanwhile, the corresponding total weight of the structure increases by only 1.6%. Following closely is the case when the height of the longitudinal girder at T0 is elevated to that of the longitudinal girder at T1 (1 200 mm), resulting in a larger increase in ultimate bearing capacity.

Table 3 Results of pillar strengthening

Pillar size/mm	Total weight of structure/kg	Ultimate bearing capacity/kN	Increase in total weight of structure/%	Increase in ultimate bearing capacity/%
Without pillar (original structure)	25 957	3 877		
150×12	26 296	4 030	1.3	3.9
250×12	26 527	4 324	2.2	11.5
350×12	26 760	4 537	3.1	17.0

Table 4 Results of longitudinal girder strengthening

Longitudinal girder size at T0/mm	Total weight of structure/kg	Ultimate bearing capacity/kN	Increase in total weight of structure/%	Increase in ultimate bearing capacity/%
450×8/150×10 (original structure)	25 957	3 877		
750×8/300×10	26 379	5 264	1.6	35.8
1000×8/300×10	26 598	4 746	2.5	22.4
1200×8/300×10	26 772	5 034	3.1	29.8

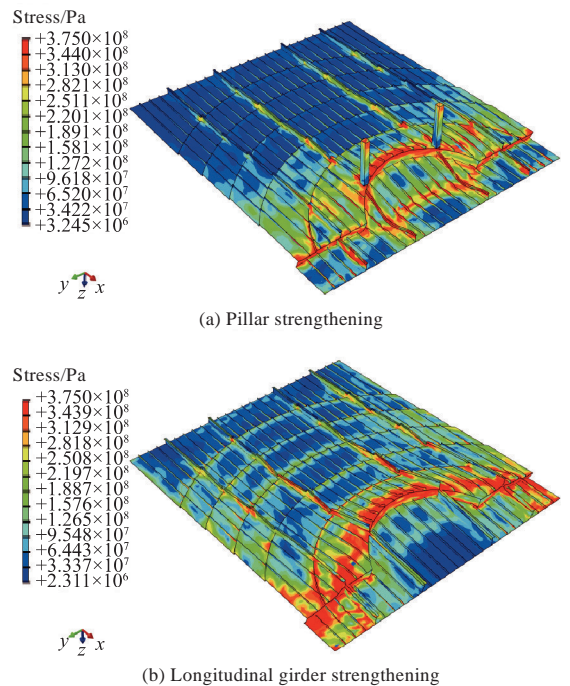


Fig. 11 Ultimate strength state of strengthening structure

4 Conclusions

This paper focuses on the unconventional stepped deck in modern cruise ships, utilizing the ABAQUS quasi-static method to calculate the structure's ultimate bearing capacity. A comparison with failure characteristics of the conventional deck is presented, along with an analysis of the effects of changes in the thickness of the deck, longitudinal, longitudinal girder web, and longitudinal girder panel. Additionally, two structural optimization ideas are proposed. The following conclusions are drawn.

1) The weak position of the stepped deck is identified as the junction of T0 and T1 with the largest height difference. During longitudinal compression, the collapse center and high-stress area are concentrated in this region, with the main yielding area distributed in a ring shape. In contrast, the compressive failure of the conventional deck exhibited a regular symmetric distribution. The primary block yielding occurred between panels, and the collapse initiated from the geometric center, radiating outward.

2) The ultimate bearing capacity of the stepped deck experiences a significant decrease, amounting to only about 20% of that of a conventional deck of equal size. Additionally, the longitudinal compression displacement corresponding to the ultimate strength state and the depth of the collapse center increase substantially.

3) The ultimate bearing capacity of the stepped deck increases with the augmentation of the thickness of decks, longitudinals, longitudinal girder webs, and longitudinal girder panels. Notably, increasing the thickness of longitudinal girder webs has the most significant improvement effect, followed by the deck plate thickness.

4) Introducing pillars at the weak position of the stepped deck or elevating the height of longitudinal girder webs at T0 can result in a slight increase in the total weight of the structure. Moreover, this enhancement effectively increases the ultimate bearing capacity. The strengthening effect becomes more pronounced with a larger pillar size. When the height of the pillar is equal to that of the T1 deck, the longitudinal girders exhibit the most effective strengthening effect.

References

[1] MEI J X, DU Z F, ZHU H T. Influencing factors of ul-

- timate strength of stiffened plate of ship structure [J]. *Ship Engineering*, 2021, 43(9): 37–42, 64 (in Chinese).
- [2] PAIK J K, SEO J K. Nonlinear finite element method models for ultimate strength analysis of steel stiffened-plate structures under combined biaxial compression and lateral pressure actions—Part I: plate elements [J]. *Thin-Walled Structures*, 2009, 47(8/9): 1008–1017.
- [3] PAIK J K, SEO J K. Nonlinear finite element method models for ultimate strength analysis of steel stiffened-plate structures under combined biaxial compression and lateral pressure actions—Part II: stiffened panels [J]. *Thin-Walled Structures*, 2009, 47(8/9): 998–1007.
- [4] CUI J J, WANG D Y, MA N. A study of container ship structures' ultimate strength under corrosion effects [J]. *Ocean Engineering*, 2017, 130: 454–470.
- [5] LIU B, GAO L J, AO L, et al. Experimental and numerical analysis of ultimate compressive strength of stiffened panel with openings [J]. *Ocean Engineering*, 2021, 220: 108453.
- [6] LIU B, YAO X N, LIN Y S, et al. Experimental and numerical analysis of ultimate compressive strength of long-span stiffened panels [J]. *Ocean Engineering*, 2021, 237: 109633.
- [7] WAN Q, WANG F H. Longitudinal stability analysis and optimum design of supportless long-span deck structure [J]. *Shipbuilding of China*, 2011, 52(1): 17–25 (in Chinese).
- [8] ZHANG J, SHI X H, GU X K. Ultimate strength study of stiffened plate under complex loading with initial imperfections [J]. *Shipbuilding of China*, 2013, 54(1): 60–70 (in Chinese).
- [9] GUO G H. Study on strength assessment method for typical bearing structure of cruise superstructure [D]. Wuhan: Wuhan University of Technology, 2019 (in Chinese).
- [10] GAN J, SHAN O, WU W G, et al. Ultimate strength analysis of typical perforated high web frame structure in cruise ships [J]. *Chinese Journal of Ship Research*, 2021, 16(5): 181–188 (in Chinese).
- [11] ZHOU H C, KONG X S, YUAN T, et al. Experimental study on the ultimate bearing capacity of deck grillage structure with multiple openings [J]. *Chinese Journal of Ship Research*, 2019, 14(2): 45–50 (in Chinese).
- [12] CCS. Rules for Classification of Sea-going Steel Ships [M]. Beijing: China Communications Press, 2018 (in Chinese).
- [13] SHI G J, GAO D W. Analysis of hull girder ultimate strength for cruise ship with multi-layer superstructures [J]. *Ships and Offshore Structures*, 2019, 14(7): 698–708.
- [14] CUI J J, WANG D Y, MA N. Key influencing factors in ultimate strength analysis for large container ships [J]. *International Journal of Offshore and Polar Engineering*, 2019, 29(1): 85–96.

邮轮非常规阶梯甲板极限承载力研究

余杨^{*1,2}, 郭虎^{1,2}, 余建星^{1,2}, 王福程^{1,2}, 张凌波^{1,2}, 苏晔凡^{1,2}

1 天津大学 建筑工程学院 水利工程智能建设与运维全国重点实验室, 天津 300072

2 天津大学 建筑工程学院 天津市港口与海洋工程重点实验室, 天津 300072

摘要: [目的] 为了探究邮轮异型甲板结构的强度底数, 针对邮轮剧院布置使用的非常规阶梯甲板进行极限承载力研究。 [方法] 基于 ABAQUS 准静态方法计算阶梯甲板的极限承载力, 确定结构的薄弱位置, 并与常规甲板失效模式进行对比, 同时探究甲板、纵骨、纵桁腹板以及纵桁面板厚度变化对结构极限承载力的影响, 提出支柱加强和纵桁加强两种结构优化方法。 [结果] 结果表明: 阶梯甲板的失效主要发生在高度差最大的层交界处, 极限承载力较常规甲板大幅下降, 对应的压缩位移和塌陷深度明显增大; 极限承载力会随甲板、纵骨、纵桁腹板以及纵桁面板厚度的增大而增大, 其中纵桁腹板厚度变化的提升效果最显著; 在结构薄弱位置增设支柱, 或增大该处纵桁腹板高度能有效提高结构的极限承载力。 [结论] 所做研究对指导现代邮轮特殊甲板的设计和优化具有重要意义。

关键词: 邮轮; 阶梯甲板; 极限承载力; 结构优化